


Quantum-state creation in nonlinear-waveguide arrays

Craig S. Hamilton,^{1,*} Regina Christ,² Sonja Barkhofen,² Stephen M. Barnett ,³ Igor Jex,¹ and Christine Silberhorn²

¹*FNSPE, Czech Technical University in Prague, Br̃hová 7, 119 15, Praha 1, Czech Republic*

²*Integrated Quantum Optics, Universität Paderborn, Warburger Strasse 100, 33098 Paderborn, Germany*

³*School of Physics and Astronomy, University of Glasgow, Glasgow G12 8QQ, United Kingdom*



(Received 22 November 2021; accepted 23 March 2022; published 29 April 2022)

Many photonic quantum information tasks employ single photons and linear transformations to create and manipulate quantum states of light to process information. Integrated optical systems have become useful platforms to perform these tasks. New technologies introduce new possible processes available for multimode quantum operations. Here we explore one such setup, motivated by current experiments, which is a nonlinear-waveguide array system operating in a regime of nondegenerate-frequency down-converted photons. This allows one photon to act as a herald for the other photon, which is created in a superposition of the individual waveguide channels. We demonstrate this setup's ability to generate highly nonclassical states, such as N -photon Fock states and NOON states.

DOI: [10.1103/PhysRevA.105.042622](https://doi.org/10.1103/PhysRevA.105.042622)

I. INTRODUCTION

Photonic states are essential parts for many tasks in quantum information processing (QIP) due to their versatility in different tasks and ease of generation and detection [1–3]. In particular, single photons are useful due to their highly non-Gaussian nature, a prerequisite for many quantum computational tasks. Typically, single-photon Fock states are generated by parametric down-conversion (PDC), where the photons are created in pairs, one of which is detected to herald the presence of its twin photon. These heralded photons can then enter subsequent optical elements that manipulate the information contained in the photonic degrees of freedom. These optical elements are generally linear transformations, with nonlinear transformations difficult to enact upon photons due to weak coupling between them, although the latter are necessary for some quantum computational operations. One way to increase the available operations is to include postselection, where part of a quantum state is measured and the remaining modes of the system are kept (for future processing) only if the desired measurement result was obtained (heralding photons is a simple example of this).

To realize these photonic operations there are many platforms that can create and transform quantum states of light. One particular platform is integrated optics, where miniaturized optical devices, such as beam splitters and phase shifters, are built into chips, which minimize losses and grant higher phase stability in the optical circuit and allow for many such components on a single chip. Coupled waveguide arrays (WGA) are an example of such an integrated optical device. These systems are constructed by altering the refractive index of an underlying material, creating channels that confine light within them and constrains it to travel along them. When

these channels are positioned close to each other, the light can couple evanescently between the channels, which can be described by a tight-binding Hamiltonian [4,5].

One version of the WGA combines the linear coupling of the channels and the nonlinear PDC, such that both processes happen concurrently (when a classical pump laser is present in at least one channel) on a single optical chip. The fundamental properties of these processes were studied [6–8] in regimes where the down-converted photons are degenerate in frequency. Moreover, this platform possesses the flexibility of waveguide sources, which can generate photons over a broad range of frequencies ranging from two-color pairs in different spectral regions [9] to spectrally indistinguishable pairs in the telecom range [10,11]. It can be driven in either the low or high gain regime, corresponding to the generation of probabilistic single pairs or squeezed states and also allows for low-loss photon operations and each mode is spatially separated for easy detection setups. State generation in this nonlinear WGA setup has been considered in the continuous variable regime of quantum optics [12–17]. There has also been experimental implementations of this setup [10,18,19].

In this work we explore a nonlinear WGA, consisting of many coupled channels, in a regime where the PDC photon pairs are highly nondegenerate in frequency. As the evanescent coupling is frequency dependent, this means that one photon (per pair) couples to neighboring waveguide channels and will evolve into a superposition of spatial modes. The other photon remains confined to the channel where it was created and is used to herald the creation of the photon pair.

We will show that this allows for the creation of nonlinear photonic states through the combination of photon generation and linear coupling and we will investigate the properties of this transfer matrix and its ability to generate states of light that are useful for QIP. We will show that this combination of the state generation and linear coupling allows for these states to be created with greater efficiency than the traditional

*hamilcra@fjfi.cvut.cz

methods of single photons entering a linear interferometer. Also, we will show that combining state generation and linear coupling gives different states when compared to these traditional methods. When compared against Gaussian states entering a linear interferometer with postselection at the output over all modes, this method does not need phase stabilization between the input modes.

Our paper is structured as follows. In Sec. II we briefly review state generation with linear optics. Next, in Sec. III, we describe the operation of the nonlinear WGA in detail and derive the transfer matrix Υ that connects the properties of the signal and herald photons. Following that, in Sec. IV, we describe how to create states useful to QIP protocols. In Sec. V, we comment on a realistic experimental implementation in the lithium niobate material platform and consider how scalable such an approach is. We conclude the paper in Sec. VI.

II. STATE CREATION THROUGH LINEAR OPTICS

Currently one of the most successful methods of creating quantum optical states is the combination of down-converted photons and linear interferometers [20,21]. The initial single-photon state is created by two-mode PDC, where in one mode a photon is detected, which heralds the presence of a photon in the other mode. These single photons then enter a linear interferometer that transforms the input modes to output modes. This interferometer is represented by unitary matrix and can be physically realized by a network of beam splitters and phase shifters when the photons are encoded in a spatial position. This process has been used to create highly entangled states of photons [22–24], which are useful for various information processing tasks. Alongside this linear transformation, postselection is used in combination with linear optics to increase the range of states or operations that can be realized. One major example of this is the KLM scheme [25] to achieve the control-phase gate using linear optics, ancilla photons, and postselection.

In the next section we describe a process where we combine the linear coupling of neighboring waveguide channels and nonlinear down-conversion. The resulting Hamiltonian is a multimode squeezing Hamiltonian, which can be controlled by pump-shaping and phase-matching processes. This will allow us to generate multimode entangled states that are not simply related by linear optics without the need for postselection.

III. WAVEGUIDE ARRAY HAMILTONIAN

In this section we describe the Hamiltonian of the WGA, which consists of linear and nonlinear terms that describe the coupling between channels and the PDC process respectively. This model is motivated by the availability of a current system in LiNbO₃ [7].

The integrated WGA consists of M coupled waveguide channels, see Fig. 1 where the process of parametric down-conversion is enabled due to the nonlinearity of the material and the periodic poling of the structure [26–28]. Photons can evanescently couple to nearest-neighbor waveguide channels at a rate that depends upon their wavelength and the distance between the channels.

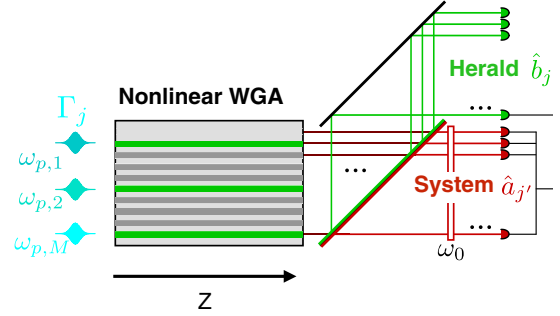


FIG. 1. System sketch. Photons from different pump frequencies $\omega_{p,j}$ decay into a nondegenerate pair of herald (800 nm) and signal (1550 nm) photons. The photons are then split at a dichroic mirror, whereafter the signal photons have to pass a narrow-band filter ($\omega_{\text{filter}} = \omega_0$). Finally the near-infrared photons are used as a herald for photons in the telecom regime.

This array coupling profile gives rise to a band structure of eigenfrequencies with corresponding eigenmodes. The Hamiltonian can be studied by calculating these eigenmodes of the linear terms (the coupling and free-rotating terms) and then transforming the PDC to this eigenmode basis. This results in a multimode squeezing Hamiltonian in the eigenmode basis whose time evolution can then be solved. The evanescent coupling of light between neighboring waveguides is heavily wavelength dependent, as shown experimentally in Ref. [7] (see Appendix A and reference therein). We will focus on a regime where the PDC photons are at nondegenerate wavelengths (\hat{b} modes are at approx. 810 nm and \hat{a} modes are at 1550 nm, as in de Chatellus *et al.* [29]). This means that the herald photons remain confined to a single waveguide channel whereas the signal photons couple coherently throughout the array. This regime has already been demonstrated in a single waveguide channel [9].

The Hamiltonian density of the WGA, which has been studied extensively in Refs. [6–8], is,

$$\begin{aligned} \hat{H}(\omega_a, \omega_b, z, t) &= \sum_{j=1}^M \beta_a(\omega_a) \hat{a}_j^\dagger \hat{a}_j + \sum_{j=1}^M \beta_b(\omega_b) \hat{b}_j^\dagger \hat{b}_j + C_a \sum_{j=1}^{M-1} \hat{a}_j^\dagger \hat{a}_{j+1} \\ &+ \int d\omega_p \sum_{j=1}^M d_j(z) \Gamma_j(\omega_p, t) \hat{a}_j^\dagger \hat{b}_j + \text{H.c.} \end{aligned} \quad (1)$$

Here the first two summations (over all M waveguide channels) describe the free rotation of the signal and herald fields, the third summation describes the linear coupling between nearest-neighbor waveguide channels of the signal fields. The operators $\hat{a}_j^\dagger, \hat{b}_j^\dagger$ (\hat{a}_j, \hat{b}_j) are the creation (annihilation) operators for the signal (herald) modes, respectively. We already assume that the herald field does not couple to the other waveguide modes to simplify the Hamiltonian. The propagation constant of the light in a single, uncoupled waveguide is denoted by $\beta_v(\omega_v)$, where ω_v is the frequency of that light, and C_a is the coupling parameter of the signal modes (at approximately $\omega_a = 1550$ nm). $\Gamma_j(\omega_p, t)$ is the time-dependent amplitude for the classical pump field, where

we assume a continuous wave source with frequency ω_p in waveguide j and is thus a delta function $\delta(\omega_p)$. The full Hamiltonian then involves all frequencies over the length of the crystal,

$$H(t) = \int_0^L dz \int d\omega_a \int d\omega_b \hat{H}(\omega_a, \omega_b, z, t). \quad (2)$$

The function $d_j(z)$ represents the periodic poling pattern of the waveguide channel, which is the domain of up- and down-poling regions. This enables the quasi-phase-matching process, which can readily be seen when $d(z)$ is written as a Fourier series [30],

$$d(z) = \sum_{n=1}^{\infty} d_n e^{i2n\pi z/\Lambda} \quad (3)$$

where Λ is the period of the poling. Usually, as an approximation, only the first term is kept for subsequent analysis. This poling pattern can be engineered to selectively phase match different eigenmodes by changing the period of the poling and in principle can take different patterns for each channel j [13]. We use this to create NOON states, as described in a future section.

The linear Hamiltonian of the \hat{a}_j modes can be diagonalized by unitary transform to the set of eigenmodes, \hat{A}_k (which are superpositions of the individual \hat{a} operators), with

$$\hat{A}_k = \sum_{j=1}^M \mu_{k,j} \hat{a}_j = \sqrt{\frac{2}{M+1}} \sum_{j=1}^M \sin\left(\frac{\pi jk}{M+1}\right) \hat{a}_j, \quad (4)$$

The corresponding eigenvalues for the k th eigenmode are given by

$$\Omega_{a,k} = \beta_a(\omega_a) + 2C_a \cos\left(\frac{k\pi}{M+1}\right), \quad (5)$$

which act as modified propagation constants for the eigenmodes [31]. The Hamiltonian density transformed to the \hat{A} -mode picture is then,

$$\begin{aligned} \hat{H}(\omega_a, \omega_b, z, t) &= \sum_{k=1}^M \Omega_{a,k} \hat{A}_k^\dagger \hat{A}_k + \sum_{j=1}^M \beta_b(\omega_b) \hat{b}_j^\dagger \hat{b}_j \\ &+ \sum_{j=1}^M d_j(z) \Gamma_j(\omega_p, t) \hat{b}_j^\dagger \sum_{k=1}^M \mu_{j,k}^* \hat{A}_k^\dagger + \text{H.c.}, \quad (6) \end{aligned}$$

where μ_{jk}^* the transformation from eigenmode to the physical basis ($\hat{a}_j = \sum_{k=1}^M \mu_{k,j}^* \hat{A}_k$). We then transform the Hamiltonian to the interaction picture to remove the free-rotating terms to arrive at,

$$\begin{aligned} \hat{H}_{\text{int}}(\omega_a, \omega_b, z, t) &= \sum_{j,k=1}^M \Gamma_j(\omega_p, t) \exp[i(\omega_{p,j} - (\omega_a + \omega_b))t] \\ &\times d_j(z) \exp[i(\beta_{p,j} - (\Omega_{a,k} + \beta_b))z] \mu_{k,j}^* \hat{A}_k^\dagger \hat{b}_j^\dagger + \text{H.c.} \quad (7) \end{aligned}$$

We now integrate $\hat{H}_{\text{int}}(z, t)$ over the z variable (from 0 to L , the length of the crystal) which leads to the phase-matching function $\Phi(\Delta\beta)$. If we assume $d_j(z)$ can be approximated with the first-order term $e^{i2\pi z/\Lambda}$ [30] this integral will yield the phase-matching function,

$$\Phi(\Delta\beta) = \int_0^L dz \exp\left[i\left(\beta_{p,j} - (\Omega_{a,k} + \beta_b) - \frac{2\pi}{\Lambda}\right)z\right]. \quad (8)$$

The phase-matching function can be written as,

$$\Phi(\Delta\beta) \propto \text{sinc}\left(\Delta\beta \frac{L}{2}\right) e^{-i\Delta\beta \frac{L}{2}}, \quad (9)$$

where

$$\Delta\beta_k(\omega_p, \omega_a, \omega_b) = \beta_p(\omega_p) - \Omega_{a,k} - \beta_b(\omega_b) - \frac{2\pi}{\Lambda}. \quad (10)$$

Phase-matched terms have $\Delta\beta = 0$ and yield a strong signal as the light evolves through the WGA. Terms that are phase mismatched oscillate and decay in relative amplitude during evolution. The desired output state can thus be created by altering the poling period Λ . We will discuss this in the next section.

The time variable is integrated over, as in Ref. [32], by extending the limits to $\pm\infty$ and we ignore time-ordering effects [33],

$$\int_{-\infty}^{\infty} dt \exp[i(\omega_p - \omega_a - \omega_b)t] = 2\pi [\delta(\omega_p - (\omega_a + \omega_b))], \quad (11)$$

which then yields the energy conservation factor [34]. This leads to perfect correlation between the signal and herald photon frequencies and modifies the pump spectral function to $\Gamma(\omega_a + \omega_b)$. As we consider a spectral function with narrow width and filter at the output at a specific frequency we can assume that only two frequencies take part in the dynamics. This simplifies the Hamiltonian as we can consider the dynamics of only two specific matching frequencies.

The combination of Γ_j and Φ will determine which pairs of modes (\hat{A}_k, \hat{b}_j) are created within the device and this can be controlled by pump shapes and periodic poling patterns. After these integrals are taken, the evolution operator, and the state at the output of the WGA, can now be written as,

$$|\psi\rangle = \exp\left[-\frac{i}{2\hbar}(\hat{M}^\dagger + \hat{M})\right]|0\rangle, \quad (12)$$

where $\hat{M}^\dagger = \sum_{j,k} M_{j,k} \hat{A}_j^\dagger \hat{b}_k^\dagger$. If we were only interested in low photon numbers we could simply expand the exponential operator perturbatively to first order. As we wish to go beyond first-order terms, we will use operator-ordering techniques [35] to allow us to write the unitary evolution operator in (12) in a normally ordered form. This means that the created state that is a multimode squeezed vacuum state, which can be written as,

$$|\Psi\rangle_{\text{out}} = \exp\left(-\frac{i}{\hbar} \sum_{k=1}^M \sum_{j=1}^M \Upsilon_{j,k} \hat{A}_k^\dagger \hat{b}_j^\dagger\right) |0\rangle \quad (13)$$

As the exponent is a quadratic operator it can be written as,

$$\frac{1}{2}[\hat{A}^\dagger, \hat{b}^\dagger] \begin{bmatrix} 0 & \Upsilon \\ \Upsilon^\dagger & 0 \end{bmatrix} \begin{bmatrix} \hat{A}^\dagger \\ \hat{b}^\dagger \end{bmatrix} = [\hat{A}^\dagger, \hat{b}^\dagger] \mathbf{T} \begin{bmatrix} \hat{A}^\dagger \\ \hat{b}^\dagger \end{bmatrix}. \quad (14)$$

We note that T is a symmetric matrix, as is necessary for the operator-ordering techniques and $[\hat{A}^\dagger, \hat{b}^\dagger] = [\hat{A}_1^\dagger, \dots, \hat{A}_M^\dagger, \hat{b}_1^\dagger, \dots, \hat{b}_M^\dagger]$ is a vector of the creation operators. The matrix T is related to M through the operator-ordering techniques [35].

At the output of the WGA we separate the signal and herald photons via a dichroic mirror. Photons in the \hat{b} mode(s) can then be measured to herald the presence of the photons in the \hat{A} modes, thereby creating states to be used for QIP. In an experimental realization we can readily implement this scheme using standard optical components. Afterwards the photons in the visible regime pass the narrow-band filter ($\omega_{\text{filter}} = \omega_b$) to ensure that they are indistinguishable in the frequency domain and interfere accordingly. In the end, we record the click patterns of the visible-spectrum photons as a heralding for the coupling photons in the telecom band.

This arrangement allows for a compact device with no interfacing losses because both processes are combined in a single chip. In addition the shorter overall length also reduces losses, as typically these scale with length.

IV. QUANTUM STATES CREATED BY WGA

In this section we describe various states that can be created from this process, starting with the direct relation to linear optics.

1. Single eigenmode per channel

The first case we consider is one designed to recreate the operation of linear optics, where we generate single-photon Fock states that are then coupled into different spatial modes of an interferometer. To do this, we phase match a single eigenmode per waveguide channel, which means that the poling period in the j th channel, Λ_j , is channel dependent,

$$\Lambda_j = 2\pi(\beta_p - \Omega_{a,j} - \beta_b)^{-1}, \quad (15)$$

which serves to phase match the j th eigenmode to the j th channel. This means that Υ is a diagonal matrix,

$$\Upsilon = \begin{bmatrix} \Upsilon_{1,1} & 0 & \dots & 0 \\ 0 & \Upsilon_{2,2} & \dots & 0 \\ \vdots & \vdots & \ddots & \vdots \\ 0 & 0 & \dots & \Upsilon_{M,M} \end{bmatrix}.$$

This means that each eigenmode only couples to one herald mode and thus after measuring the herald photons in the set of modes $\{k\}$ we have prepared the state of telecom photons,

$$|\psi\rangle = \frac{1}{\mathcal{N}} \prod_{\{k\}} \Upsilon_{k,k} \hat{A}_k^\dagger |0\rangle \rightarrow \prod_{\{k\}} \hat{A}_k^\dagger |0\rangle, \quad (16)$$

where \mathcal{N} is a normalization constant. The magnitude of each $\Upsilon_{k,k}$ is not important, as the postselection effect is to remove these factors after normalization. However, we assume that the Υ should be within an order of magnitude of each other to ensure suitable postselection rates. The signal photons here are created in the eigenmode basis and not the usual physical

basis and are therefore already in a superposition of physical modes, which may be useful for QIP depending upon the transformation μ .

2. N -photon Fock states

We next show how this process can be used to create N -photon Fock states. These states can be created with linear optics albeit with a probability that decreases exponentially, either due to the nature of single-photon generation or interfering multiple noninteracting photons, such that exit in the same mode [36–38]. Here we present a method that avoids the latter cost, simply leaving the generation probability of N photons, which can be increased by pumping multiple waveguide channels.

We can create N -photon Fock states by phase matching the same eigenmode, say \hat{A}_1^\dagger , in each channel, i.e., the poling period is channel independent, $\Lambda_j \equiv \Lambda$. This may not be possible in every channel due to zero overlap between some channels and the desired eigenmodes, i.e., $\mu_{j,k} = 0$, which is a function of the coupling configuration. The state at the output is

$$|\psi\rangle = \exp\left(-\frac{i}{\hbar} \hat{A}_1^\dagger \sum_j \Upsilon_j \hat{b}_j^\dagger\right) |0\rangle, \quad (17)$$

where Υ is,

$$\Upsilon = \begin{bmatrix} \Upsilon_{1,1} & \Upsilon_{1,2} & \dots & \Upsilon_{1,N} \\ 0 & 0 & \dots & 0 \\ \vdots & \vdots & \ddots & \vdots \\ 0 & 0 & \dots & 0 \end{bmatrix}.$$

When we measure photons in any of the \hat{b} modes we will have created a photon in the eigenmode \hat{A}_1 and due to the nature of the phase matching all the photons created are in this eigenmode. Photon number resolving detectors may be necessary to properly distinguish the output states and increase the fidelity of the device, and will also allow for \hat{b} photons in the same mode to contribute to the N -photon Fock state. Placing a multimode interferometer that enacts the transformation μ at the output of the WGA, the state will be converted from the eigenmode basis, $\{\hat{A}\}$, to the physical basis, $\{\hat{a}\}$, yielding the N -photon Fock state in that basis.

N -photon Fock states can also be created probabilistically by multiplexing single-photon sources [39] from linear optics. Using the optimal interferometer [36], it was shown that the probability to create such a state scales as $\text{Pr}(N) \approx N!/N^N \approx e^{-N}$ for large N . This ignores the probability to generate the initial N single-photon states, which will scale as p^N , where p is the probability to generate a photon pair from PDC. The total probability to generate the output state is therefore $\approx (p/e)^N$.

We create our desired state after coherent, unitary time evolution and herald only on photon detection events as opposed to both pair creation events and the correct multiplexed output of photons from the device. The main benefit of this is that it eliminates the probabilistic creation of the N -photon state from the N single photons (with e^{-N} scaling), leaving the generation probability of the N photons. This can be seen from the Bloch-Messiah decomposition of the matrix \mathbf{T} (that

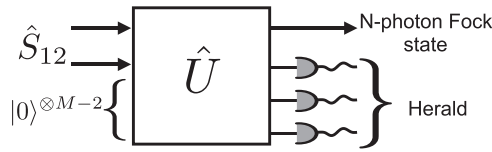


FIG. 2. Schematic of the Bloch-Messiah decomposition into a set of single-mode squeezers followed by a linear interferometer. \hat{S}_{12} is the operator for the SMSS, which have identical squeezing parameter, r .

describes the state), which shows that it is equivalent to a two-mode squeezed state, which can create an N -photon Fock state when conditioned on measuring N herald photons in the other channel. The difference in our state is that the N herald photons are spread over more channels.

As the operator, (17), is quadratic we can decompose it using the Bloch-Messiah decomposition into a set of initial single-mode squeezed states followed by a linear interferometer, see Fig. 2. When we decompose this Hamiltonian we find that it is equivalent to two single-mode squeezed states (with identical squeezing parameters) followed by a linear interferometer. This input state can also be written as a two-mode squeezed state (TMSS), which has recently been used to create N -photon Fock states [38]. The probability to generate $2N$ photons (herald and signal photons) is then given by the photon number distribution from a TMSS, which is $\text{Pr}(2N) = \sinh^{2N} r$ [40].

3. NOON states

Another class of states that can be created in a similar fashion are the NOON states,

$$|\phi\rangle = |N, 0\rangle + |0, N\rangle = (\hat{A}_1^{\dagger N} - \hat{A}_2^{\dagger N})|0\rangle, \quad (18)$$

which can be factorized, into N terms, as,

$$\hat{A}_1^{\dagger N} - \hat{A}_2^{\dagger N} = \prod_{j=0}^{N-1} (\hat{A}_1^{\dagger} + e^{ij2\pi/N} \hat{A}_2^{\dagger}), \quad (19)$$

where the phases correspond to the N th roots of unity.

This state can be created in the WGA by changing the periodic poling, $d_j(z)$, during the waveguide channel [13]. One way to achieve this is to phase match the first eigenmode, \hat{A}_1 , and then change the poling period to phase match the second eigenmode \hat{A}_2 . This changes the phase-matching condition and therefore what eigenmodes are created in the PDC process. The relative phase between each eigenmode, $e^{i\phi_j}$, can be adjusted by shifting the patterns relative to each other and is different in each channel. The relative phase of terms between channels [i.e., terms in the expansion (19)] is not important, in the same way it is not important between single Fock states entering an interferometer. The shape of the Υ matrix is,

$$\Upsilon = \begin{bmatrix} \Upsilon_{1,1} & \Upsilon_{1,2} & 0 & \dots & 0 \\ \Upsilon_{2,1} & \Upsilon_{2,2} & 0 & \dots & 0 \\ \vdots & \vdots & \ddots & \vdots & \\ \Upsilon_{N,1} & \Upsilon_{N,2} & 0 & \dots & 0 \end{bmatrix}$$

with $\Upsilon_{j,1} = 1$ and $\Upsilon_{j,2} = e^{i\phi_j}$.

$$\begin{aligned} \hat{M} &= \sum_{k,j} \Upsilon_{k,j} \hat{A}_k^{\dagger} \hat{b}_j^{\dagger} \\ &= \sum_j (\hat{A}_1^{\dagger} + e^{i\phi_j} \hat{A}_2^{\dagger}) \hat{b}_j^{\dagger}. \end{aligned} \quad (20)$$

When we decompose the matrix \mathbf{A} via the Bloch-Messiah decomposition we find that this requires four single-mode squeezed states with identical squeezing parameters. As before with the N -photon states, the NOON state is created in the eigenmode basis and so we must transform the photons back to the physical basis.

V. PROSPECTS FOR EXPERIMENTAL IMPLEMENTATION AND SOURCES OF ERROR

The main challenge for the experimental implementation of state generation with a nonlinear-waveguide array is the requirement on the involved pumping scheme, which we need to create the correct output state. The unique source of error in the state creation process described above is the production of other, unwanted eigenmodes of the system that can occur as these terms have low, nonzero, phase mismatch. These non-phase-matched terms oscillate in amplitude, which may not be zero at the output of the device, due to the finite length of the WGA. This will create extra terms in the Hamiltonian and thus the matrix Υ , in addition to the desired phase-matched terms. These errors stem from the spectral width σ_p of the pump function, $\Gamma(\omega_p)$, and the width of the phase-matching functions $\Phi(k_a, \omega_a)$ for the various eigenmodes. In this section we investigate the necessary requirements to realize this scheme using current technology.

To illustrate the source of errors in state creation, we will consider a WGA chip with constant coupling between nearest neighbor waveguides, i.e., $C_{j,j+1} = C$ and nine WGA channels. We filter at a particular frequency ω_b . The eigenfrequencies are given by (5), and the spatial, quasimomentum part that defines the eigenmodes is given by,

$$2C \cos\left(\frac{k\pi}{M+1}\right). \quad (21)$$

To ensure that we only pump the desired combination of signal, herald frequencies (ω_a, ω_b) and eigenmode(s) in each waveguide, the width of the phase-matching function, $\Delta\omega_{PM}$ has to be lower than the frequency gap between neighboring eigenmodes, $\Delta_{j,j+1} = |\Omega_j - \Omega_{j+1}|$. This can be realized by having a sufficiently long crystal, as the phase-matching function Φ decays with length, as can be seen in Eq. (9). This condition coupled with a narrow spectral pump function gives two constraints on the three variables and finally filtering selects the desired set.

The spectral gap between nearest-neighbor eigenmodes is

$$\begin{aligned} \Delta_{j,j+1} &= |\beta_j - \beta_{j+1}| = 4C \sin\left(\frac{(2j+1)\pi}{2(M+1)}\right) \sin\left(\frac{1}{2} \frac{\pi}{M+1}\right) \\ &\approx \frac{2C\pi}{M+1} \sin\left(\frac{(2j+1)\pi}{2(M+1)}\right). \end{aligned} \quad (22)$$

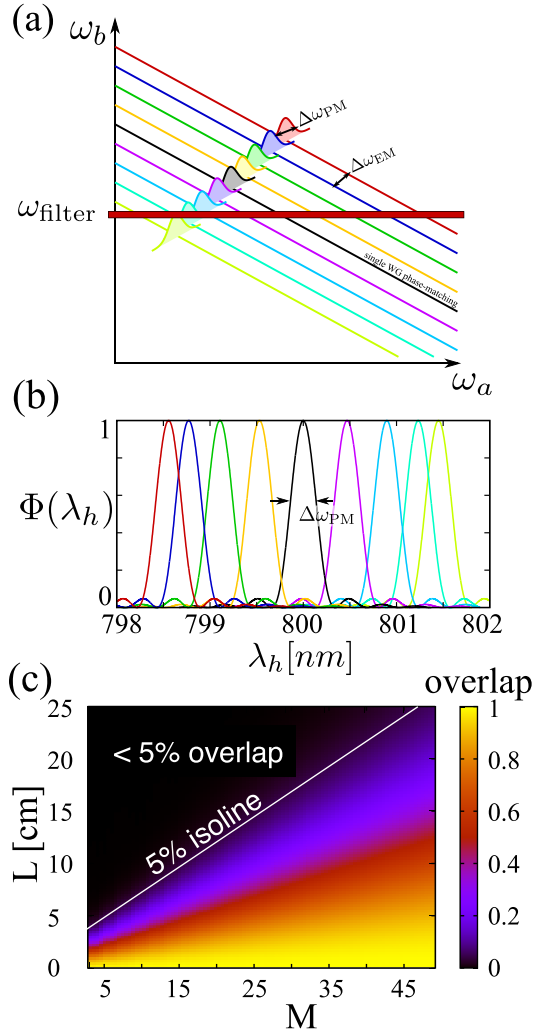


FIG. 3. Challenges for the experimental implementation. In (a), we sketch a schematic of the phase-matching conditions for the nonlinear-waveguide array. The finite width of the single phase-matching conditions causes an overlap between different eigenmodes. This limits the possibility to pump single eigenmodes in different waveguides. In (b), we compare the spectral eigenmode separation (top) to the expected phase-matching widths (bottom). The left to right ordering of the peaks in (b) corresponds to the top to bottom ordering in (a) of the lines. Consequently, (c) shows the expected overlap between the $(\frac{M}{2})$ th and the $(\frac{M}{2} + 1)$ th eigenmode phase matching in Gaussian approximation. The 5% limit gives a measure how much we can pump different eigenmodes separately. For details concerning calculation parameters, see text.

The amplitude of the phase-matching term for the second eigenmode is then given by $\text{sinc}(\Delta_{1,2}L/2)$, where L is the length of the crystal. The sinc function can be approximated by a Gaussian $\approx \exp[-0.193(\Delta_{1,2}L/2)^2]$ [41]. It can be seen that when the number of waveguides, M , is increased then $\Delta_{1,2}$ decreases and the length of the crystal must be increased to maintain the phase gap at a constant value.

We illustrate these ideas in a series of figures. We consider an implementation in lithium niobate [10,42], using the relevant refractive indices and an experimentally feasible coupling parameter of $C_s = 350 \text{ m}^{-1}$. In Fig. 3(a) we

show the phase-matching curves [Eq. (10), $\Delta\beta_j = 0 \forall j$] for each of different eigenmodes. Also shown is a sketch of the phase-matching functions with spectral width $\Delta\omega_{PM}$ for each eigenmode. We then filter at the frequency ω_{filter} , which takes a cross section of the eigenmodes phase-matching functions, shown in Fig. 3(b). The spectral separation of the different eigenmodes $\Delta_{1,2}$ is primarily dependent on the number of channels in the WGA and secondarily on the band structure of the array, which is determined by the coupling parameters of the array. The width of a single phase-matching function $\Delta\omega_{PM}$, is then determined by this separation $\Delta_{j,j+1}$ and the length of the array, L .

In Fig. 3 we have plotted the different eigenmode phase-matching functions for an array of $L = 0.04 \text{ m}$ and the above-mentioned array parameters. From this figure it becomes clear that we should expect a significant overlap at least for the outer phase-matching functions. To quantify this effect for the inner phase-matching conditions (i.e., the best-case scenario), we have calculated the overlap between neighboring phase-matching functions [i.e., the black and violet curve of Fig. 3(b)] using the Gaussian approximation above.

To illustrate the scalability of our system, we have varied both the length L of the WGA, as well as the number of waveguides M , to calculate the overlap, as shown in Fig. 3(c). As can be seen from the 5% isoline, we have to increase the length of the sample linearly with the number of waveguides to keep the overlap between two phase-matching functions fixed to below a certain value. As current technology restricts the maximum possible length of the WGA to $L_{\text{max}} \approx 10 \text{ cm}$, this analysis suggests 15–20 waveguides could be utilised in an experimental implementation.

Another factor that contributes to the error of unwanted mode creation is given by the transformation matrix μ . Ideally the matrix elements $\mu_{j,k}$, which relates the pumped waveguide channel k to the eigenmodes j , would be zero for those unwanted modes. Different coupling configurations of the waveguide channels ($C_{j,j+1}$) will have different transformations matrices μ and thus this is parameter that can be optimized for any particular experiment.

VI. CONCLUSION

In conclusion, we have proposed the use of a different arrangement of coupled waveguide array channels with an intrinsic nonlinearity to create quantum states of light. We do so by using the nonlinear behavior of the phase-matching process that occurs during the generation of light in each channel to create states that are not simply created with linear optics alone. We showed that our setup has several advantages compared to previous schemes. The classes of states that can be generated with our scheme cover higher-order Fock states as well as NOON states. The experimental implementation at least for moderate number of waveguides, is possible with current available technology. In addition, the idea of using phase matching with postselection will be applicable to other nonlinear optical systems and platforms.

ACKNOWLEDGMENTS

C.S.H. and I.J. received support from the Ministry of Education RVO 68407700 and ÖCentre for Advanced

Applied Sciences, Registry No. CZ.02.1.01/0.0/0.0/16_019/0000778, supported by the Operational Programme Research, Development and Education, cofinanced by the European Structural and Investment Funds and the state budget of the Czech Republic. The Integrated Quantum

Optics group (IQO) acknowledges financial support through the Gottfried Wilhelm Leibniz-Preis (Grant No. SII115/3-1) and the European Commission through the ERC project QuPoPCoRN (Grant No. 725366). S.M.B thanks the Royal Society for support (RP 150122).

- [1] P. Kok, W. J. Munro, K. Nemoto, T. C. Ralph, J. P. Dowling, and G. J. Milburn, *Rev. Mod. Phys.* **79**, 135 (2007).
- [2] J. Wang, F. Sciarrino, A. Laing, and M. G. Thompson, *Nature Photon.* **14**, 273 (2020).
- [3] S. Slussarenko and G. J. Pryde, *Appl. Phys. Rev.* **6**, 041303 (2019).
- [4] D. N. Christodoulides, F. Lederer, and Y. Silberberg, *Nature (London)* **424**, 817 (2003).
- [5] I. L. Garanovich, S. Longhi, A. A. Sukhorukov, and Y. S. Kivshar, *Phys. Rep.* **518**, 1 (2012).
- [6] A. S. Solntsev, A. A. Sukhorukov, D. N. Neshev, and Y. S. Kivshar, *Phys. Rev. Lett.* **108**, 023601 (2012).
- [7] R. Kruse, F. Katzschmann, A. Christ, A. Schreiber, S. Wilhelm, K. Laiho, A. Gábris, C. S. Hamilton, I. Jex, and C. Silberhorn, *New J. Phys.* **15**, 083046 (2013).
- [8] A. S. Solntsev, F. Setzpfandt, A. S. Clark, C. W. Wu, M. J. Collins, C. Xiong, A. Schreiber, F. Katzschmann, F. Eilenberger, R. Schiek, W. Sohler, A. Mitchell, C. Silberhorn, B. J. Eggleton, T. Pertsch, A. A. Sukhorukov, D. N. Neshev, and Y. S. Kivshar, *Phys. Rev. X* **4**, 031007 (2014).
- [9] S. Krapick, H. Herrmann, V. Quiring, B. Brecht, H. Suche, and C. Silberhorn, *New J. Phys.* **15**, 033010 (2013).
- [10] R. Kruse, L. Sansoni, S. Brauner, R. Ricken, C. S. Hamilton, I. Jex, and C. Silberhorn, *Phys. Rev. A* **92**, 053841 (2015).
- [11] L. Sansoni, K. H. Luo, C. Eigner, R. Ricken, V. Quiring, H. Herrmann, and C. Silberhorn, *npj Quantum Inf.* **3**, 5 (2017).
- [12] A. Rai and D. G. Angelakis, *Phys. Rev. A* **85**, 052330 (2012).
- [13] J. G. Titchener, A. S. Solntsev, and A. A. Sukhorukov, *Phys. Rev. A* **92**, 033819 (2015).
- [14] D. Barral, N. Belabas, L. M. Procopio, V. D'Auria, S. Tanzilli, K. Bencheikh, and J. A. Levenson, *Phys. Rev. A* **96**, 053822 (2017).
- [15] D. Barral, K. Bencheikh, V. D'Auria, S. Tanzilli, N. Belabas, and J. A. Levenson, *Phys. Rev. A* **98**, 023857 (2018).
- [16] J. G. Titchener, A. S. Solntsev, and A. A. Sukhorukov, *Phys. Rev. A* **101**, 023809 (2020).
- [17] D. Barral, M. Walschaers, K. Bencheikh, V. Parigi, J. A. Levenson, N. Treps, and N. Belabas, *Phys. Rev. A* **102**, 043706 (2020).
- [18] F. Setzpfandt, A. S. Solntsev, J. Titchener, C. W. Wu, C. Xiong, R. Schiek, T. Pertsch, D. N. Neshev, and A. A. Sukhorukov, *Laser Photon. Rev.* **10**, 131 (2016).
- [19] X. Guo, C.-I. Zou, C. Schuck, H. Jung, R. Cheng, and H. X. Tang, *Light Sci. Appl.* **6**, e16249 (2017).
- [20] J.-W. Pan, Z.-B. Chen, C.-Y. Lu, H. Weinfurter, A. Zeilinger, and M. Żukowski, *Rev. Mod. Phys.* **84**, 777 (2012).
- [21] J. Carolan, C. Harrold, C. Sparrow, E. Martín-López, N. J. Russell, J. W. Silverstone, P. J. Shadbolt, N. Matsuda, M. Oguma, M. Itoh *et al.*, *Science* **349**, 711 (2015).
- [22] C. K. Law, I. A. Walmsley, and J. H. Eberly, *Phys. Rev. Lett.* **84**, 5304 (2000).
- [23] J. Romero, D. Giovannini, S. Franke-Arnold, S. M. Barnett, and M. J. Padgett, *Phys. Rev. A* **86**, 012334 (2012).
- [24] J. Peřina, *Phys. Rev. A* **92**, 013833 (2015).
- [25] E. Knill, R. Laflamme, and G. J. Milburn, *Nature (London)* **409**, 46 (2001).
- [26] W. H. Louisell, A. Yariv, and A. E. Siegman, *Phys. Rev.* **124**, 1646 (1961).
- [27] M. Fejer, G. Magel, D. H. Jundt, and R. Byer, *IEEE J. Quantum Electron.* **28**, 2631 (1992).
- [28] S. Tanzilli, H. De Riedmatten, H. Tittel, H. Zbinden, P. Baldi, M. De Micheli, D. Ostrowsky, and N. Gisin, *Electron. Lett.* **37**, 26 (2001).
- [29] H. G. de Chatellus, A. V. Sergienko, B. E. A. Saleh, M. C. Teich, and G. di Giuseppe, *Opt. Express* **14**, 10060 (2006).
- [30] D. S. Hum and M. M. Fejer, *C. R. Phys.* **8**, 180 (2007).
- [31] C. Kittel, *Introduction to Solid State Physics*, 8th ed. (Wiley, New York, 2004).
- [32] W. P. Grice and I. A. Walmsley, *Phys. Rev. A* **56**, 1627 (1997).
- [33] A. Christ, B. Brecht, W. Mauerer, and C. Silberhorn, *New J. Phys.* **15**, 053038 (2013).
- [34] R. W. Boyd, *Nonlinear Optics* (Academic Press, San Diego, 1992).
- [35] X. Ma and W. Rhodes, *Phys. Rev. A* **41**, 4625 (1990).
- [36] O. Steuernagel, *Opt. Commun.* **138**, 71 (1997).
- [37] K. R. Motes, R. L. Mann, J. P. Olson, N. M. Studer, E. A. Bergeron, A. Gilchrist, J. P. Dowling, D. W. Berry, and P. P. Rohde, *Phys. Rev. A* **94**, 012344 (2016).
- [38] J. Tiedau, T. J. Bartley, G. Harder, A. E. Lita, S. W. Nam, T. Gerrits, and C. Silberhorn, *Phys. Rev. A* **100**, 041802(R) (2019).
- [39] E. Meyer-Scott, C. Silberhorn, and A. Migdall, *Rev. Sci. Instrum.* **91**, 041101 (2020).
- [40] S. Barnett and P. M. Radmore, *Methods in Theoretical Quantum Optics* Vol. 15 (Oxford University Press, Oxford, 2002).
- [41] A. B. U'Ren, C. Silberhorn, R. Erdmann, K. Banaszek, W. P. Grice, I. A. Walmsley, and M. G. Raymer, *Las. Phys.* **15**, 146 (2005).
- [42] D. H. Jundt, *Opt. Lett.* **22**, 1553 (1997).